

# Tetrahydrohyperforin prevents cognitive deficit, A $\beta$ deposition, tau phosphorylation and synaptotoxicity in the APP<sup>swe</sup>/PSEN1 $\Delta$ E9 model of Alzheimer's disease: a possible effect on APP processing

NC Inestrosa<sup>1</sup>, C Tapia-Rojas<sup>1</sup>, TN Griffith<sup>1,4</sup>, FJ Carvajal<sup>1</sup>, MJ Benito<sup>2</sup>, A Rivera-Dictter<sup>3</sup>, AR Alvarez<sup>2</sup>, FG Serrano<sup>1</sup>, JL Hancke<sup>1</sup>, PV Burgos<sup>3</sup>, J Parodi<sup>1</sup> and L Varela-Nallar<sup>1</sup>

Alzheimer's disease (AD) is a neurodegenerative disorder characterized by a progressive deterioration of cognitive abilities, amyloid- $\beta$  peptide (A $\beta$ ) accumulation and synaptic alterations. Previous studies indicated that hyperforin, a component of the St John's Wort, prevents A $\beta$  neurotoxicity and some behavioral impairments in a rat model of AD. In this study we examined the ability of tetrahydrohyperforin (IDN5607), a stable hyperforin derivative, to prevent the cognitive deficit and synaptic impairment in an *in vivo* model of AD. In double transgenic APP<sup>swe</sup>/PSEN1 $\Delta$ E9 mice, IDN5706 improves memory and prevents the impairment of synaptic plasticity in a dose-dependent manner, inducing a recovery of long-term potentiation. In agreement with these findings, IDN5706 prevented the decrease in synaptic proteins in hippocampus and cortex. In addition, decreased levels of tau hyperphosphorylation, astrogliosis, and total fibrillar and oligomeric forms of A $\beta$  were determined in double transgenic mice treated with IDN5706. In cultured cells, IDN5706 decreased the proteolytic processing of the amyloid precursor protein that leads to A $\beta$  peptide generation. These findings indicate that IDN5706 ameliorates AD neuropathology and could be considered of therapeutic relevance in AD treatment.

*Translational Psychiatry* (2011) 1, e20; doi:10.1038/tp.2011.19; published online 12 July 2011

## Introduction

Alzheimer's disease (AD) is characterized by a progressive deterioration of cognitive abilities, eventually leading to the death of the individual. Accumulation of the amyloid- $\beta$  peptide (A $\beta$ ), a product of the processing of the amyloid precursor protein (APP), is believed to have a key role in the cognitive deficits observed in AD.<sup>1</sup> Although, the mechanisms involved in the pathogenic changes triggered by A $\beta$  are not clearly understood, the neuronal dysfunction and cytoskeletal alterations are early manifestations that lead to aberrant remodeling of dendrites and axons, synaptic loss,<sup>2</sup> and eventually progressive loss of neuronal populations,<sup>3</sup> which is associated with the appearance of dystrophic neurites and abnormal phosphorylation of cytoskeletal proteins mostly phosphorylation of the microtubule-associated protein tau.<sup>3,4</sup> Besides, analyses of AD mouse models and AD patients brains support the hypothesis that aggregates of A $\beta$  are responsible for the 'synaptic failure', which occurs before the plaque development and neuronal cell death; such effects are triggered by A $\beta$  oligomers, which are soluble and toxic molecular forms of A $\beta$ .<sup>5,6</sup> The synaptic failure is correlated

with the reduction in synaptic proteins and alterations in synaptic function.<sup>7–11</sup>

Hyperforin, the active molecule for the anti-depressant activity of St John's Wort (*Hypericum perforatum*)<sup>12</sup> has been suggested to have the capacity to enhance memory in rodents.<sup>13</sup> Previously, we had shown that hyperforin reduces the behavioral alteration induced by intra-hippocampal injection of A $\beta$  fibrils in an acute rat model of AD.<sup>14</sup> Tetrahydrohyperforin (IDN5706) a semi synthetic derivative of hyperforin, with a higher stability and increased oral bioavailability,<sup>15</sup> has also shown some neuroprotective properties.<sup>16</sup>

In this study, we examined the effects of IDN5706 *in vivo* on A $\beta$  neurotoxicity using young transgenic mice APP<sup>swe</sup>/PSEN1 $\Delta$ E9 in order to seek whether or not we can prevent the development of the neuropathology. Five-month-old transgenic mice were treated for 10 weeks, tested for spatial memory and their brains were used for biochemical, histochemical and electrophysiological analysis. We report here that IDN5706 significantly reduces the spatial memory impairments, tau hyperphosphorylation, A $\beta$  oligomer accumulation and increases long-term potentiation (LTP),

<sup>1</sup>Centro de Envejecimiento y Regeneración (CARE), Santiago, Chile; <sup>2</sup>Departamento de Biología Celular y Molecular, Facultad de Ciencias Biológicas, P. Universidad Católica de Chile, Santiago, Chile and <sup>3</sup>Instituto de Fisiología, Facultad de Medicina, Universidad Austral de Chile, Valdivia, Chile

Correspondence: Dr NC Inestrosa, CARE Center P. Universidad Católica de Chile, Santiago 8331150, Chile.

E-mail: ninestrosa@bio.puc.cl

<sup>4</sup>Present address: Graduate School, Neuroscience PhD Program, Northwestern University, Evanston, IL.

**Keywords:** APP transgenic; A $\beta$  neurotoxicity; *Hypericum perforatum*; IDN5706; LTP; PHF-1 phosphorylation

Received 2 June 2011; accepted 3 June 2011

suggesting the availability of a new pharmacological tool to fight against AD.

## Materials and methods

**Reagents and antibodies.** Tetrahydroperforin (IDN5706) was obtained from Indena SpA, Milan, Italy. Tetrahydroperforin is a semi synthetic derivative of hyperforin (WO 03/091194 A1; WO 2004/106275 A2). Primary antibodies used are as follows: rabbit anti-gial fibrillar acidic protein (DAKO, Denmark), mouse anti-A $\beta$  (4G8, Chemicon, Temecula, CA, USA), goat anti-synaptophysin, rabbit polyclonal anti- $\beta$ -tubulin, rabbit anti-tubulin (Santa Cruz Biotechnology, Santa Cruz, CA, USA) and mouse anti tau epitope paired-helical filament1 (PHF-1). The monoclonal antibodies anti-PSD95, anti-NR2B and anti-VGlu1 were developed by and obtained from the UC Davis/NIH NeuroMab Facility (Davis, CA, USA).

**Animals.** APP<sup>swe</sup>/PSEN1 $\Delta$ E9 mice, which express the mutant APP<sub>SWE</sub> (K595N/M596L) and PSEN1 $\Delta$ E9, deletion of the exon 9 (APP-PS1 mice stock 004462) were obtained from Jackson Laboratory (Bar Harbor, ME, USA). Treatments were performed by i.p. injection of IDN5706 with solutol as vehicle, initiated at 5 months of age and continued three times a week per 10 weeks. Transgenic and wild-type control animals were injected with the vehicle.

**Behavioral test.** The Morris water maze was performed as previously described in our laboratory.<sup>17,18</sup>

**Slice preparation and electrophysiology.** Hippocampal slices were prepared according to the standard procedures previously described in our laboratory.<sup>19</sup> To generate LTP we used high-frequency stimulation (HFS), three trains of 500 ms stimuli at 100 Hz with a 20-s interval. Recordings were filtered at 2.0–3.0 kHz, sampled at 4.0 kHz using an A/D converter, and stored with pClamp 10 (Molecular Devices, Sunnyvale, CA, USA). Evoked postsynaptic responses were analyzed off-line, using an analysis software (pClampfit, Molecular Devices), which allowed visual detection of events, computing only those events that exceeded an arbitrary threshold.

**Immunohistochemical procedures.** Perfusion, fixation and free-floating immunohistochemical procedures were performed as previously described.<sup>17,18,20</sup> Image analysis and PHF-1 neuronal counting were carried out as previously described.<sup>17,20</sup>

**Thioflavine S (ThS) staining.** ThS staining was developed in sections mounted on gelatin-coated slices as previously described.<sup>17,18</sup>

**Immunoblotting.** The hippocampus and cortex of treated or control transgenic mice were dissected on ice and immediately frozen at  $-150^{\circ}\text{C}$  or processed. Immunoblotting and slot blot assays were performed as previously described.<sup>17,21</sup>

**H4 neuroglioma transfection.** For C99-EGFP, the sequence encoding C99 with a signal peptide was cloned by PCR using as a template C99-GFP kindly provided by Dr Christian Haass and cloned in frame into *Xho*I and *Sal*I sites of pEGFP-N1. Transfections of H4 neuroglioma cells were carried out using Lipofectamine 2000 (Invitrogen, Carlsbad, CA, USA) for 1 h at  $37^{\circ}\text{C}$  in the absence of FBS and 16 h post-transfection cells were incubated at different times with 100–500  $\mu\text{M}$  IDN-5706, 250 nM DAPT (Sigma-Aldrich, St Louis, MO, USA), 150  $\mu\text{g ml}^{-1}$  CHX (Sigma-Aldrich) and 40  $\mu\text{g ml}^{-1}$  chloramphenicol (Sigma-Aldrich).

**Statistical analysis.** Data analysis was carried out with Prism software (GraphPad Software, La Jolla, CA, USA). Results were expressed as mean  $\pm$  s.e. For statistical analysis, normally distributed data were analyzed by one-way ANOVA with *post hoc* tests performed using the Tukey test. Non-normally distributed data were analyzed by the Kruskal–Wallis test with *post hoc* tests performed using Dunn's test.

## Results

**IDN5706 treatment decreased A $\beta$  burden, tau hyperphosphorylation and astrogliosis in double transgenic APP<sup>swe</sup>/PSEN1 $\Delta$ E9 mice.** Double transgenic mice that express the mutant APP<sub>SWE</sub> (K595N/M596L) and PS1 (PSEN1 $\Delta$ E9: deletion of the exon 9) generate A $\beta$  plaques in both the cortex and hippocampus in an age- and region-dependent manner.<sup>22</sup> To analyze the effect of IDN5706 on physiopathological markers of AD, 5-month-old double transgenic APP<sup>swe</sup>/PSEN1 $\Delta$ E9 mice (APP-PS1) were injected i.p. with 4 mg kg<sup>-1</sup> IDN5706 or vehicle (control) three times a week per 10 weeks. By staining with an antibody against total A $\beta$ , we first analyzed A $\beta$  burden in the cortex and hippocampus (Figure 1a). A significant reduction in A $\beta$  burden was observed in IDN5706-treated mice as measured by the area positive for A $\beta$  aggregates (Figure 1b). IDN5706 also decreased the amount of A $\beta$  sheet burden measured by ThS staining (Supplementary Figure 1). These results indicate that IDN5706 prevents A $\beta$  load in the transgenic mouse model.

Apparently, A $\beta$  oligomers are responsible for the synaptic dysfunction observed in AD patients and mice models.<sup>5</sup> We determined the relative amount of A $\beta$  oligomers by slot blot using the specific antibody A11 as previously described.<sup>23</sup> Brain extracts from APP-PS1 mice treated with 4 mg kg<sup>-1</sup> IDN5706 for 10 weeks showed a reduction in the relative amount of A $\beta$  oligomers in both hippocampus and cortex compared with control APP-PS1 mice injected with the vehicle solution (Figure 1c), indicating that IDN5706 reduces the amount of synaptotoxic A $\beta$  oligomers present in AD mice brains.

The phosphorylation of tau, particularly the appearance of the epitope PHF-1 (phosphorylated Ser-396 and Ser-404), was analyzed nearby A $\beta$  plaques stained with ThS (Figure 1d). Although tau phosphorylation affects different parts of the hippocampus and cortex, we choose to evaluate PHF-1-positive cells in a circular area ( $r = 100 \mu\text{m}$ ) surround-

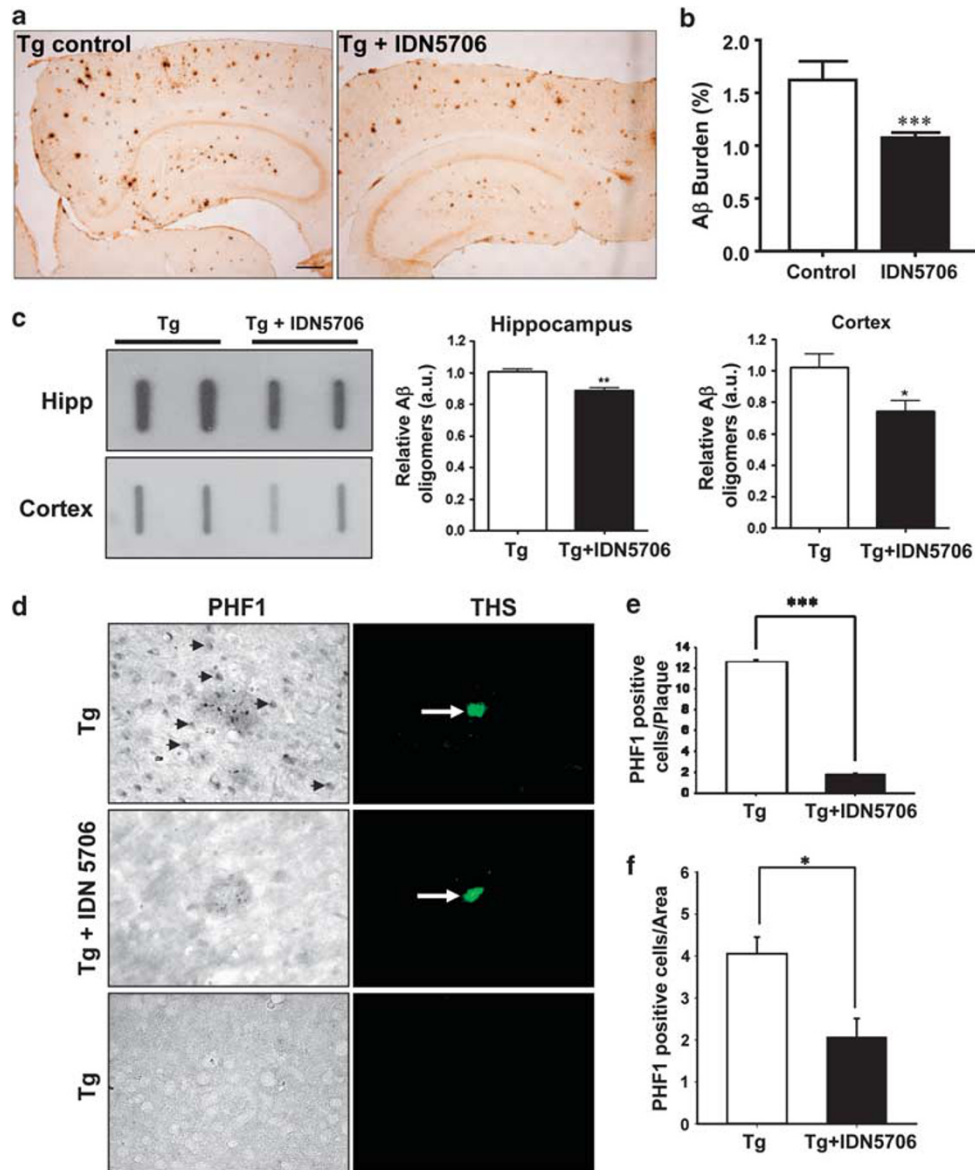


**Figure 1** IDN5706 reduces the total amount of A $\beta$ , the levels of A $\beta$  oligomers and the number of PHF-1-positive neurons in brains of APP-PS1 mice. (a) Total A $\beta$  aggregates in control APP-PS1 transgenics (Tg control) and in IDN5706-treated brains (Tg + IDN5706). Tg control mice were injected i.p. with vehicle solution and Tg + IDN5706 were injected with 4 mg kg<sup>-1</sup> IDN5706 three times a week per 10 weeks. (b) Average area fraction positive for A $\beta$ . Bars represent the average plaque area for the treatment  $\pm$  s.e. ( $n = 4$ ). (c) Representative slot blot from hippocampal and cortical fractions using 6  $\mu$ g protein per slot spotted into a nitrocellulose membrane and expose to A11 antibody. Graphs represent normalized densitometric analysis profile of the slot intensity for each treatment. (d) Images show representative detection of PHF-1-positive cells (left panels) near amyloid plaques detected with ThS (right panels). Positive neurons are indicated by black arrows and the amyloid plaques by a white arrow. Bottom panels show that no PHF-1-positive cells are detected in other regions. (e, f) The graphs show the quantification of the number of PHF-1-positive neurons per plaque (e) and per area in 0.03 mm<sup>2</sup> (f). Bars represent the mean  $\pm$  s.e. ( $n \geq 3$ ). \* $P < 0.05$ ; \*\* $P < 0.01$ ; \*\*\* $P < 0.001$ .

ing amyloid plaques<sup>20</sup> as it has been described that cytoskeletal changes, tau phosphorylation, glial fibrillar acidic protein activation and synapses loss occurs mainly in these areas.<sup>2,20,24</sup> Treatment with IDN5706 induced ~an 80% decrease in the number of PHF-1-positive neurons next to amyloid deposits (Figures 1d, middle panels, and Figure 1e). Although few PHF-1-positive cells were found outside the circular area around the plaques (Figure 1d, bottom panels), we analyzed total PHF-1-positive cells per area (cortex + hippocampus) and determined a strong decrease by IDN5706 treatment (Figure 1f).

The astroglial inflammatory reaction is another pathological change characteristic of AD brains.<sup>25</sup> APP-PS1 mice show higher staining for the marker of astroglial inflammatory reaction glial fibrillar acidic protein than age-matched wild-type animals (Supplementary Figure 2A), and this staining was significantly reduced in the hippocampus and cortex of IDN5706-treated APP-PS1 mice. IDN5706 treatment also reduced perikaryon enlargement in hippocampus (Supplementary Figure 2B) and cortex (Supplementary Figure 2C), indicating that IDN5706 prevents the neuro-inflammatory reaction characteristic of AD.

A $\beta$  burden and tau phosphorylation was also evaluated in APP-PS1 mice injected i.p. with different concentrations of IDN5706. Treatment with 2, 4 and 6 mg kg<sup>-1</sup> IDN5706 reduced A $\beta$  burden, as assessed by staining with an antibody against total A $\beta$  (Figures 2a and b) and A $\beta$  sheet burden measured by ThS staining (Figure 2c and Supplementary Figure 3). Tau phosphorylation in Ser-396 and Ser-404 (PHF-1 antibody) and in Ser-202 residue (AT8 antibody) was assessed by immunoblotting. A dose-dependent decrease

in both epitopes was observed in the hippocampi of APP-PS1 mice (Figure 2d). In agreement with the reduced phosphorylation of tau, treatment with IDN5706 increased the levels of the inactive form of GSK-3 $\beta$  that is phosphorylated in serine 9 residue (Figure 2e).

**Treatment with IDN5706 enhances the spatial learning in wild-type mice and prevents the spatial memory loss in APP-PS1 mice.** The effect of IDN5706 on hippocampal

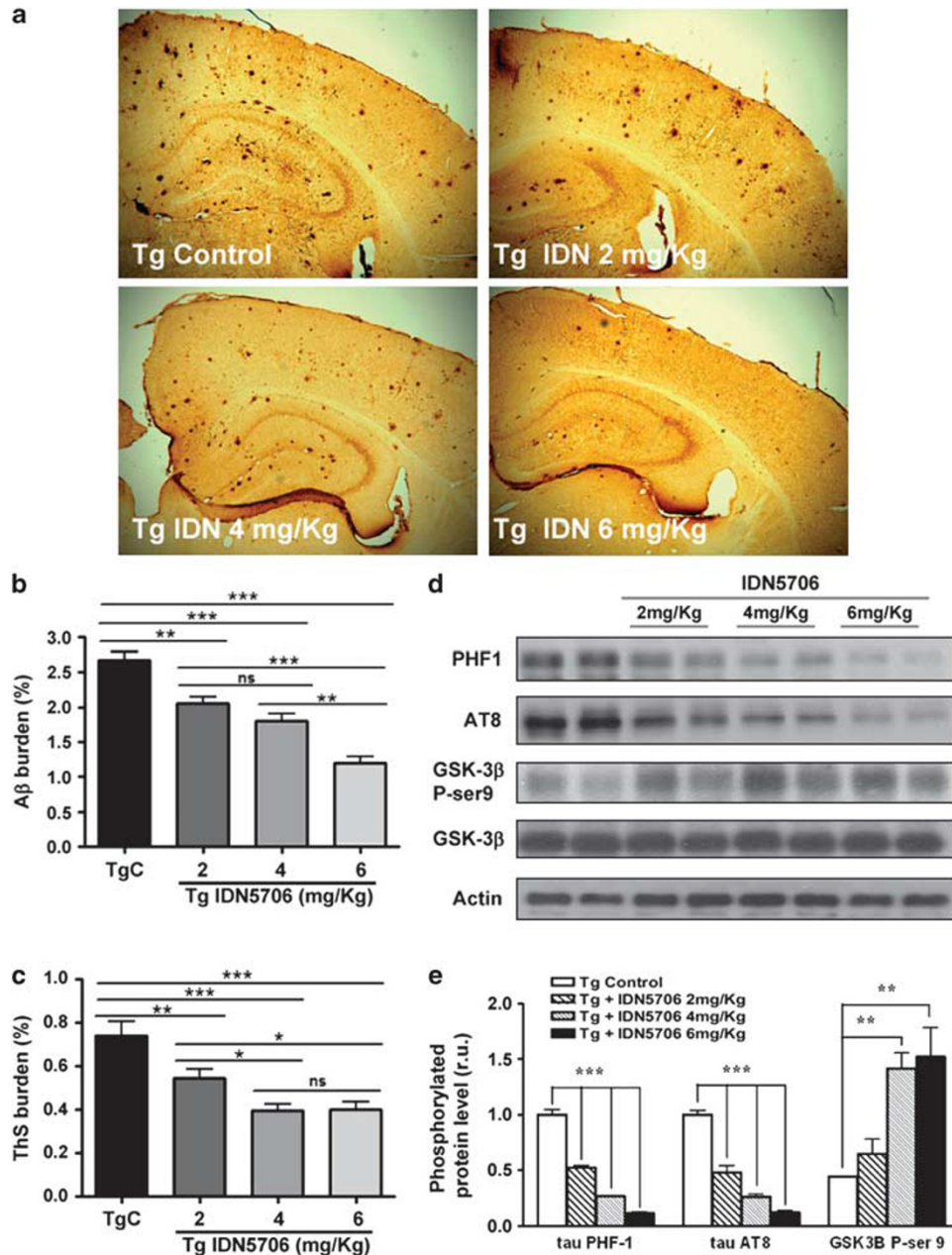


**Figure 2** Dose-dependent decrease of A $\beta$  deposits and tau phosphorylation in APP-PS1 mice. (a) Total A $\beta$  aggregates in control APP-PS1 transgenics (Tg control) and in Tg treated with 2, 4 and 6 mg kg<sup>-1</sup> IDN5706 for 10 weeks. (b, c) Average area fraction positive for A $\beta$  (b) or amyloid plaques detected with ThS staining (c) in brains of control and IDN5706-treated APP-PS1 mice. (d) Immunoblot of total brain homogenates from APP-PS1 mice injected i.p. with vehicle solution or 2, 4 and 6 mg kg<sup>-1</sup> IDN5706 three times a week per 10 weeks using the PHF-1 and AT8 antibody. (e) The graph shows the densitometric analysis of bands normalized against  $\beta$ -actin and compared with control APP-PS1. Total and phosphorylated GSK-3 $\beta$  was also detected. The levels of GSK-3 $\beta$  phosphorylated in serine 9 were normalized against total GSK-3 $\beta$  levels. Bars represent the mean  $\pm$  s.e. ( $n \geq 3$ ). \* $P < 0.05$ ; \*\* $P < 0.01$ ; \*\*\* $P < 0.001$ .

function was assessed in APP-PS1 mice that were injected i.p. with different doses of IDN5706 or vehicle since 5-month-old, three times a week per 10 weeks. Hippocampal function was assessed in the Morris water maze spatial memory test.<sup>26</sup> In this task, mice are required to learn the location of a hidden platform by external cues. Wild-type animals treated with IDN5706 presented lower escape latency values compared with wild-type controls injected with the vehicle solution (Figure 3a). These differences were significant only during the first week of training, which indicates an improvement in the short-term memory (Figure 3b). On the other hand, APP-PS1 mice treated with all concentrations of IDN5706 showed lower latency times to reach the platform than control APP-PS1 mice (Figure 3c, Supplementary Table 1). There was a concentration-dependent decrease in the escape latency, being in animals treated with 6 mg kg<sup>-1</sup> almost similar to that of wild-type animals (Figure 3c). The behavioral improvement was observed after 4 and 5 days of testing (short-term memory) and also between 8 and 10 days (long-term memory). This effect is also observed in the distance of the swimming path to reach the platform (Figure 3d, Supplementary Table 2). APP-PS1 mice treated with IDN5706 had a significantly reduced swimming path than control APP-PS1 mice, suggesting an improvement in the hippocampal function. These results indicate that IDN5706 is able to prevent the deficit in spatial memory that appeared in APP-PS1 transgenic mice and in a dose-dependent manner.

**IDN5706 induces an increase in LTP in hippocampal slices from transgenic mice.**

The behavioral improvement in the Morris water maze could be explained by an effect of IDN5706 on synaptic activity, it is likely possible that there is a recovery or generation of a robust LTP. We explored the effects of IDN5706 on field excitatory postsynaptic potentials (fEPSP), in hippocampal slices incubated with different concentrations of IDN5706. LTP was generated using HFS (100 hz, 500 ms, three times). In APP-PS1 mice, a decreased response to the HFS was observed compared with age-matched wild-type animals (Figure 4a). A dose-dependent recovery of LTP was observed in transgenic mice treated with IDN5706. Slices from mice treated with 2 and 4 mg kg<sup>-1</sup> IDN5706 show fEPSP similar to 8-month-old wild-type animals (Figure 4a). Moreover, slices from transgenic animals treated with 6 mg kg<sup>-1</sup> IDN5706 show a stronger LTP than wild-type hippocampal slices of 8-month-old mice (Figure 4b). These results suggest that IDN5706 facilitates LTP induction in double transgenic APP-PS1 mice.

**IDN5706 prevents the decrease in synaptic proteins.**

Synaptic disturbances are present in AD brains, as well as in transgenic AD models.<sup>7,8,11,27</sup> We carried out a detailed analysis of synaptic proteins affected in APP-PS1 mice. As presynaptic markers, the levels of the synaptic vesicle protein synaptophysin and VGlut1 were evaluated.<sup>28</sup> As postsynaptic markers, the levels of the NMDA receptor subunit NR2B, the AMPA receptor subunit GluR2 and the

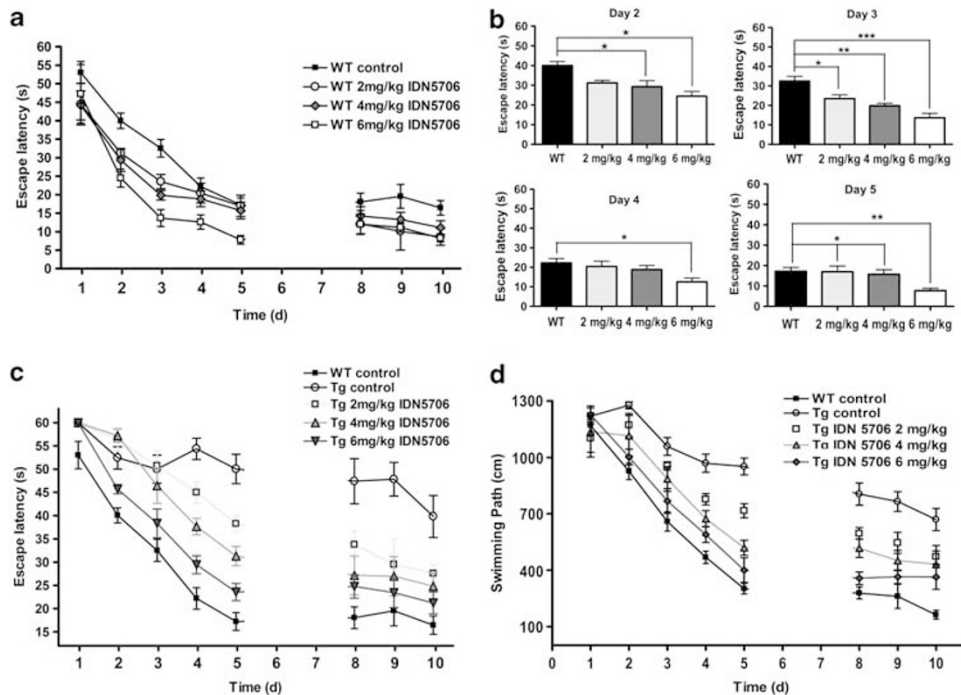


**Figure 3** Treatment with IDN5706 enhances the spatial learning in wild-type mice and reduces the spatial memory impairment in APP-PS1 mice. Mice were injected i.p. with vehicle solution or 2, 4 and 6 mg kg<sup>-1</sup> IDN5706 three times a week per 10 weeks. Spatial memory was evaluated in the Morris water maze. (a) Escape latency of wild-type mice to reach the hidden platform was reduced by IDN5706 treatment. (b) The statistical analysis of escape latency of wild-type mice shows significant differences in the first weeks of training. (c) Higher escape latency during the test was shown by control APP-PS1 compared with vehicle-injected wild-type animals, and the escape latency was reduced in IDN5706-treated animals in a dose-dependent manner. (d) Analysis of the swimming path of APP-PS1 mice compared with wild-type animals. Reduced distances to reach the platform were observed in APP-PS1 mice treated with increasing doses of IDN5706. Statistical analyses are shown in Supplementary Tables 1 and 2. \**P* < 0.05; \*\**P* < 0.01; \*\*\**P* < 0.001.

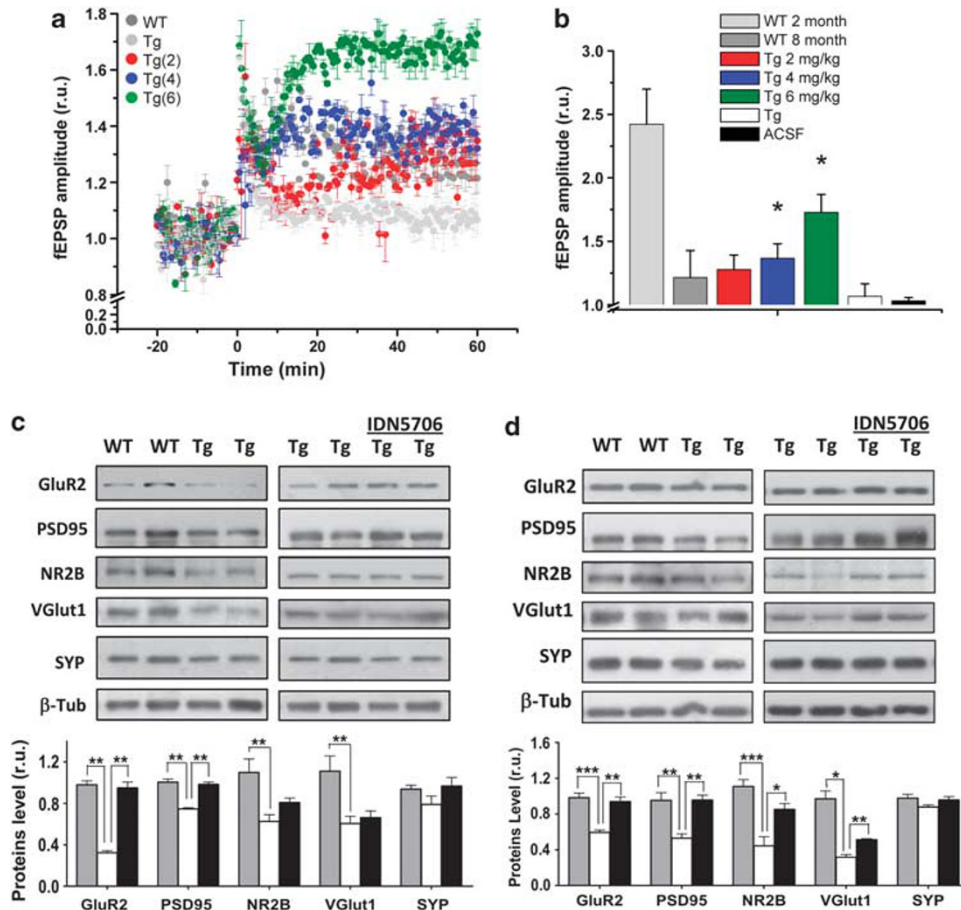


**Figure 4** IDN5706 improves LTP in hippocampal slices from APP-PS1 mice in a dose-dependent manner and prevents the reduction of synaptic proteins in APP-PS1 mice. **(a)** LTP generated by HFS in hippocampal slices from wild-type mice, control APP-PS1 and APP-PS1 mice treated with 2, 4 or 6 mg kg<sup>-1</sup> of IDN5706. Quantification of fEPSP amplitude is shown. **(b)** Plot of fEPSP amplitude after 60 min of HFS in hippocampal slices from wild-type mice, control APP-PS1 and APP-PS1 mice treated with 2, 4 or 6 mg kg<sup>-1</sup> of IDN5706. The graph shows the mean  $\pm$  s.e from six independent experiments. \**P* < 0.05, compared with APP-PS1 mice. **(c, d)** Representative immunoblots of total protein extracts from hippocampus **(c)** and cortex **(d)** of wild-type (WT, gray bars) and APP-PS1 (Tg, white bars) and APP-PS1 mice treated with IDN5706 (black bars). Graphs correspond to the densitometric analysis of each protein normalized against  $\beta$ -tubulin and compared with the levels of the same protein in WT mice (*n* = 4). \**P* < 0.05; \*\**P* < 0.01; \*\*\**P* < 0.001.

postsynaptic density protein PSD-95 were evaluated.<sup>29</sup> APP-PS1 animals show reduced levels of most of the synaptic proteins evaluated (VGlut1, GluR2, PSD-95 and NR2B) in the hippocampus and cortex as compared with age-matched wild-type animals (Figures 4c,d). Treatment with IDN5706 prevented the decrease of postsynaptic markers observed in APP-PS1 mice. In the hippocampus of IDN5706-treated animals there was a significant protection in total levels of GluR2 and PSD-95 (Figure 4c), while the cortex showed higher levels of these two proteins and also of NR2B and VGlut1 (Figure 4d). These results indicate that IDN5706 is able to prevent the synaptic protein loss observed in APP-PS1 mice.

**IDN-5706 inhibits C99  $\gamma$ -secretase proteolytic processing.** Finally, and in an attempt to explore the potential mechanism involved in the neuroprotective effect of IDN5706, we analyzed whether IDN5706 affects the proteolytic processing that leads to A $\beta$  peptide generation. Because a small percentage of APP is cleaved by

$\beta$ -secretase, we examined the effect of IDN5706 using a recombinant EGFP-tagged C99 construct (C99-EGFP) that mimics  $\beta$ -secretase-cleaved APP. This system conveniently allows us to characterize all proteolytic events that tightly control C99 levels and thus, A $\beta$  peptide generation. This includes: (i)  $\gamma$ -secretase cleavage that results in release of A $\beta$  into the extracellular space and of the APP intracellular domain (AICD $\gamma$ ) into the cytosol; (ii)  $\alpha$ -secretase cleavage that mediates conversion of C99 to C83, thus reducing A $\beta$  peptide production; (iii) and caspase cleavage leading to the production of cytosolic C31 (Figure 5a). Immunoblotting for C99-EGFP in H4 neuroglioma cells, a well-established model system for biochemical analysis of C99 processing,<sup>30</sup> showed four species corresponding to C99, C83, AICD $\gamma$  and C31 (Figure 5b). This result indicates that this construct is indeed processed by all the corresponding enzymatic activities, confirming our previous findings<sup>30</sup> (Figure 5b). Increasing concentrations of IDN5706 for 8 h resulted in a dramatic decrease in AICD $\gamma$  levels (Figure 5b). At 100  $\mu$ M IDN5706, AICD $\gamma$  decreased to a 40% the level present in

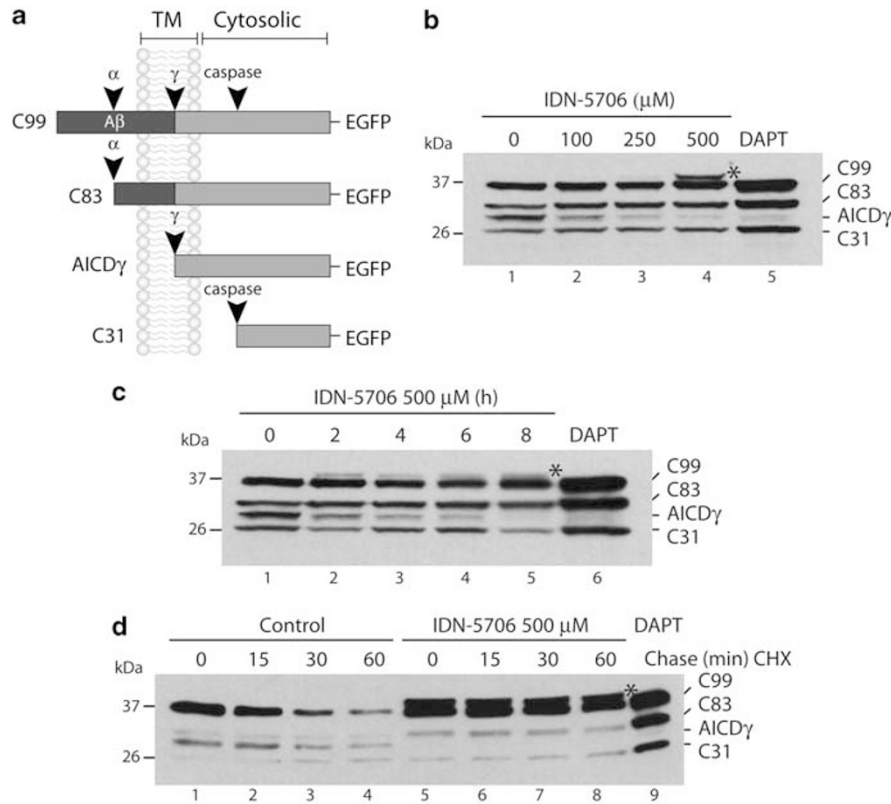


**Figure 5** IDN5706 inhibits C99 proteolytic processing by  $\gamma$ -secretase in H4 neuroglioma cells. **(a)** Schematic representation of C99 indicating its topological domains; the position of the A $\beta$  peptide; the  $\alpha$ ,  $\gamma$ , and caspase cleavage sites; and the fragments produced. **(b, c)** Anti-GFP immunoblot analysis from H4 neuroglioma cells transfected with EGFP-tagged C99 after treatment with only IDN5706 with the variations indicated below, or in the presence of a combination of 150  $\mu\text{g ml}^{-1}$  CHX and 40  $\mu\text{g ml}^{-1}$  chloramphenicol for 0–60 min. **(d)** The positions of molecular mass markers and different proteolytic species are indicated.

untreated cells, with a maximum decrease to a 6% in cells incubated with 500  $\mu\text{M}$  IDN5706. Cells incubated with 500  $\mu\text{M}$  IDN5706 at different times showed that after 2 h AICD $\gamma$  generation decreased 40%, with the greatest reduction between 6 and 8 h (Figure 5c). This reduction in AICD $\gamma$  level was similar to that obtained with 250 nM DAPT, a specific inhibitor of  $\gamma$ -secretase activity (Figure 5c). No significant effect on the levels of C83 and C31 was observed (Figures 5b,c). Because it is well known that  $\gamma$ -secretase inhibition by DAPT leads to a delay in C99 turnover, we studied whether treatment with IDN5706 might also produce a similar outcome. H4 neuroglioma cells expressing C99-EGFP were preincubated with 500  $\mu\text{M}$  IDN5706 for 8 h and then a combination of cycloheximide and chloramphenicol was added to stop translation at different periods of time, with or without 500  $\mu\text{M}$  IDN5706 (Figure 5d). Control cells showed a short half-life of 20 min for C99 (Figure 5d, lanes 1–4). In contrast, treatment with IDN5706 resulted in a dramatic delay in the turnover of C99 (Figure 5d, lanes 5–8). Altogether these data suggest that IDN5706 affects the processing of C99 probably by inhibition of  $\gamma$ -secretase cleavage.

## Discussion

In this study, we have demonstrated that 5-month-old APP-PS1 mice treated with tetrahydrohyperforin, IDN5706,

during 10 weeks did not present decreased cognitive capacities and neuropathological markers of AD as compared with control vehicle-injected APP-PS1 mice. Specific neuroprotective effects of IDN5706 observed in this study include: reduction in total fibrillar and oligomeric forms of A $\beta$ , reduction in the levels of tau hyperphosphorylation and astrogliosis, and prevention of synaptic protein loss. Moreover, in IDN5706-treated animal it was possible to induce LTP by HFS. In neuroglioma cells, IDN5706 reduced the processing of APP that conducts to A $\beta$  peptide generation. Taken together, our data indicate that IDN5706 might be of therapeutic relevance in AD.

A previous study in our laboratory indicated that IDN5706 was able to reduce neuropathological markers in 12-month-old APP-PS1 mice treated with 2 mg kg $^{-1}$  IDN5706 for 1 month.<sup>16</sup> However, in that study no reduction in total A $\beta$  burden was found, despite a slight reduction in the size of ThS-positive plaques. In the present work, in 5-month-old APP-PS1 mice treated with 4 mg kg $^{-1}$  IDN5706 for 10 weeks, a reduction in the amount of total A $\beta$  burden, A $\beta$  amyloid plaques and A $\beta$  oligomers was found. Moreover, a dose-dependent decrease in A $\beta$ -burden was observed. Our findings suggest that treatment of young animals with IDN5706, previously to the time frame where the plaque formation takes place,<sup>31</sup> affects the mechanism of A $\beta$  peptide formation and/or its aggregation kinetics, resulting in a decreased A $\beta$  burden and lower levels of A $\beta$  oligomeric

species. Interestingly, in neuroglioma cells we determined that IDN5706 decreased the processing of APP particularly the processing by  $\gamma$ -secretase, supporting that the decrease in A $\beta$  formation might be related to the mechanism of IDN5706 neuroprotection. Another possibility that could also explain the effect of IDN5706 *in vivo* could be an enhanced clearance or disassembly of A $\beta$  aggregates. In fact, we have previously demonstrated that IDN5706 inhibits A $\beta$  aggregation *in vitro*.<sup>14</sup> Moreover, we have shown that *in vitro*, hyperforin is able to disaggregate pre-formed fibrils into protofibrils and amorphous material.<sup>14</sup> Taking into consideration our results, we think that IDN5706 might have anti-amyloidogenic actions both *in vitro* and also *in vivo*. Because IDN5706 was able to decrease the levels of oligomeric species of A $\beta$ , its anti-amyloidogenic mechanism did not result in a more toxic end products. Although we have shed light into the mechanism of action of IDN5706, further *in vivo* studies are necessary to fully clarify the molecular and cellular mechanisms involved in the reduction of A $\beta$  aggregates by IDN5706.

In our study, IDN5706 was also shown to prevent tau pathology, a key hallmark of AD.<sup>32–34</sup> Fibrils composed of hyper-phosphorylated tau accumulate within neuronal cell bodies and dendrites in AD brain and form the PHFs that coalesce into neurofibrillary tangles (NFTs). The propensity of hyper-phosphorylated tau to aggregate and binds with lower affinity to MTs suggests that reducing tau phosphorylation in AD might provide therapeutic benefits. We determined that IDN5706 reduced the number of neurons positive for PHF-1 antibody and the total amounts of tau phosphorylated at epitopes PHF-1 and AT8 in APP-PS1 mice brains. The reduction of PHF-1-positive neurons could be a consequence of a decreased accumulation of A $\beta$  and inflammatory response, and also IDN5706 may have effects on the signaling that define to trigger tau phosphorylation. Several kinases can phosphorylate tau *in vitro*; however, the bulk of the information supports that GSK-3 $\beta$ , Cdk5, extracellular signal-related kinase 2 and microtubule affinity-regulating kinase are the most relevant kinases for tau phosphorylation *in vivo*.<sup>35–37</sup> It is therefore possible that IDN5706 may be able to regulate the activity of kinases such as GSK-3 $\beta$  and Cdk5. Consistent with the role of GSK-3 $\beta$ , we found increased levels of inactive GSK-3 $\beta$  in APP-PS1 mice treated with IDN5706.

The inhibition of the signaling associated to neuronal damage has been shown to attenuate A $\beta$  accumulation. For example, the inhibition of GSK-3 $\beta$  by lithium not only reduces tau phosphorylation *in vitro* and in AD mice, but also produces a concomitant reduction in A $\beta$  production.<sup>38,39</sup> Besides, GSK-3 $\beta$  is a negative modulator of the canonical Wnt signaling pathway.<sup>40</sup> We have previously shown decreased activity of GSK-3 $\beta$  in hippocampal neurons exposed to A $\beta$  in the presence of a Wnt ligand<sup>41</sup> or the pharmacological activator of the Wnt pathway lithium,<sup>42</sup> and in APP-PS1 mice exposed to lithium.<sup>17</sup> In all these cases the inactivation of the kinase was correlated with increased Wnt activity and neuroprotection. Whether the neuroprotective effect of IDN5706 is associated to the activation of the Wnt signaling pathway will have to be determined.

The A $\beta$  oligomers can negatively modulate synaptic plasticity and memory,<sup>8</sup> generating failures and damage in the synaptic cleft.<sup>43</sup> Previously, we showed that hippocampal

slices exposed to A $\beta$  oligomers generate a synaptotoxic effect with reduced synaptic efficacy and impaired synaptic transmission mainly by decreasing NMDA and AMPA receptors currents, which could be explained by reduced levels of PSD-95 and synaptic contacts.<sup>44</sup> Our present findings indicate a positive effect of IDN5706 on LTP induction in APP-PS1 mice. LTP is a synaptic process that occurs in dendritic spines of neurons involved in synaptic plasticity related to memory in some regions of the brain.<sup>45</sup> Different reports have suggested a relationship between memory tests and LTP,<sup>46–48</sup> therefore it is possible that the improvement of LTP phenomenon could account for the recovery in the spatial memory of transgenic mice treated with IDN5706.

Finally, IDN5706 prevented the reduction of synaptic proteins *in vivo*, which is a pathological characteristic found in various AD models.<sup>9,49–51</sup> IDN5706 mainly prevented the reduction in relevant postsynaptic proteins. Interestingly, hyperforin, the compound from which IDN5706 is derived, has various neurobiological effects (for review, see ref. 52) which could explain the protective effect of IDN5706 against the synaptotoxicity observed in AD mice. For example, it is known that A $\beta$  oligomers decrease the levels of PSD-95 *in vitro*,<sup>50</sup> and we observed that IDN5706 decreased the amount of A $\beta$  oligomers *in vivo* and also decreased the processing of APP that leads to the generation of A $\beta$  peptide *in vitro*, which might explain why IDN5706 exerts protective effects over PSD-95 levels.

As mentioned, IDN5706 is a semi synthetic derivative of hyperforin which is the major active compound of SJW.<sup>52</sup> Whether hyperforin has the same neuroprotective effects determined for IDN5706 will have to be determined in future experiments. However, IDN5706 was chosen from a spectrum of derivatives due to its higher stability and because of an increased oral bioavailability as compared with hyperforin and its other derivatives,<sup>15</sup> thus this molecule is therapeutically more attractive than hyperforin itself.

In summary, our findings indicate that IDN5706 is able to reduce the neuropathology in APP-PS1 mice decreasing all the neuropathological hallmarks studied. More importantly, IDN5706 ameliorates the impairment of memory and synaptic plasticity associated to AD pathology. These findings strongly suggest a therapeutic potential of IDN5706 for the treatment of AD.

## Conflict of interest

The authors declare no conflict of interest.

**Acknowledgements.** We would like to thank Dr Peter Davies (Department of Pathology, Albert Einstein College of Medicine, NY, USA) for his kindly gift of the mouse anti-tau antibody epitope PHF-1 and Dr Christian Haass (German Center for Neurodegenerative Diseases, Ludwig-Maximilians-University, Munich, Germany) for the C99-GFP construct. This work was supported by Grants from FONDEF (N° D0711052) and the Basal Center of Excellence in Aging and Regeneration (CONICYT-PFB12/2007) to NCI, FONDECYT (N°1080221) to ARA, FONDECYT (N°1100027) to PVB and Insertion of Postdoctoral Researchers in the Academy CONICYT (N°79090027) to LV-N.

1. Selkoe DJ. Alzheimer's disease: genes, proteins, and therapy. *Physiol Rev* 2001; **81**: 741–766.
2. Tsai LH, Lee MS, Cruz J. Cdk5, a therapeutic target for Alzheimer's disease? *Biochim Biophys Acta* 2004; **1697**: 137–142.



3. Dickson DW. Apoptotic mechanisms in Alzheimer neurofibrillary degeneration: cause or effect? *J Clin Invest* 2004; **114**: 23–27.
4. Takashima A, Noguchi K, Sato K, Hoshino T, Imahori K. Tau protein kinase I is essential for amyloid  $\beta$ -protein-induced neurotoxicity. *Proc Natl Acad Sci USA* 1993; **90**: 7789–7793.
5. Haass C, Selkoe DJ. Soluble protein oligomers in neurodegeneration: lessons from the Alzheimer's amyloid  $\beta$ -peptide. *Nat Rev Mol Cell Biol* 2007; **8**: 101–112.
6. Cerpa W, Dinamarca MC, Inestrosa NC. Structure-function implications in Alzheimer's disease: effect of A $\beta$  oligomers at central synapses. *Curr Alzheimer Res* 2008; **5**: 233–243.
7. Inestrosa NC, Toledo EM. The role of Wnt signaling in neuronal dysfunction in Alzheimer's disease. *Mol Neurodegener* 2008; **3**: 9.
8. Shankar GM, Li S, Mehta TH, Garcia-Munoz A, Shepardson NE, Smith I *et al*. Amyloid- $\beta$  protein dimers isolated directly from Alzheimer's brains impair synaptic plasticity and memory. *Nat Med* 2008; **14**: 837–842.
9. Lacor PN, Buniel MC, Furlow PW, Clemente AS, Velasco PT, Wood M *et al*. A $\beta$  oligomer-induced aberrations in synapse composition, shape, and density provide a molecular basis for loss of connectivity in Alzheimer's disease. *J Neurosci* 2007; **27**: 796–807.
10. Parodi J, Sepulveda FJ, Roa J, Opazo C, Inestrosa NC, Aguayo LG. Beta-amyloid causes depletion of synaptic vesicles leading to neurotransmission failure. *J Biol Chem* 2010; **285**: 2506–2514.
11. Terry RD, Masliah E, Salmon DP, Butters N, DeTeresa R, Hill R *et al*. Physical basis of cognitive alterations in Alzheimer's disease: synapse loss is the major correlate of cognitive impairment. *Ann Neurol* 1991; **30**: 572–580.
12. Singer A, Wonnemann M, Muller WE. Hyperforin, a major antidepressant constituent of St. John's Wort, inhibits serotonin uptake by elevating free intracellular Na<sup>+</sup>. *J Pharmacol Exp Ther* 1999; **290**: 1363–1368.
13. Klusa V, Germane S, Noldner M, Chatterjee SS. Hypericum extract and hyperforin: memory-enhancing properties in rodents. *Pharmacopsychiatry* 2001; **34**(Suppl 1): S61–S69.
14. Dinamarca MC, Cerpa W, Garrido J, Hancke JL, Inestrosa NC. Hyperforin prevents  $\beta$ -amyloid neurotoxicity and spatial memory impairments by disaggregation of Alzheimer's amyloid- $\beta$ -deposits. *Mol Psychiatry* 2006; **11**: 1032–1048.
15. Rozio M, Fracasso C, Riva A, Morazzoni P, Caccia S. High-performance liquid chromatography measurement of hyperforin and its reduced derivatives in rodent plasma. *J Chromatogr B Analyt Technol Biomed Life Sci* 2005; **816**: 21–27.
16. Cerpa W, Hancke JL, Morazzoni P, Bombardelli E, Riva A, Marin PP *et al*. The hyperforin derivative IDN5706 occludes spatial memory impairments and neuropathological changes in a double transgenic Alzheimer's mouse model. *Curr Alzheimer Res* 2010; **7**: 126–133.
17. Toledo EM, Inestrosa NC. Activation of Wnt signaling by lithium and rosiglitazone reduced spatial memory impairment and neurodegeneration in brains of an APPsw/PSEN1DeltaE9 mouse model of Alzheimer's disease. *Mol Psychiatry* 2010; **15**: 272–285.
18. Chacon MA, Barria MI, Soto C, Inestrosa NC. Beta-sheet breaker peptide prevents Abeta-induced spatial memory impairments with partial reduction of amyloid deposits. *Mol Psychiatry* 2004; **9**: 953–961.
19. Varela-Nallar L, Alfaro IE, Serrano FG, Parodi J, Inestrosa NC. Wingless-type family member 5A (Wnt-5a) stimulates synaptic differentiation and function of glutamatergic synapses. *Proc Natl Acad Sci USA* 2010; **107**: 21164–21169.
20. Cancino GI, Toledo EM, Leal NR, Hernandez DE, Yevens LF, Inestrosa NC *et al*. ST1571 prevents apoptosis, tau phosphorylation and behavioural impairments induced by Alzheimer's beta-amyloid deposits. *Brain* 2008; **131**: 2425–2442.
21. McLaurin J, Kierstead ME, Brown ME, Hawkes CA, Lamberton MH, Phinney AL *et al*. Cyclohexanehexol inhibitors of A $\beta$  aggregation prevent and reverse Alzheimer phenotype in a mouse model. *Nat Med* 2006; **12**: 801–808.
22. Garcia-Alloza M, Robbins EM, Zhang-Nunes SX, Purcell SM, Betensky RA, Raju S *et al*. Characterization of amyloid deposition in the APPsw/PS1dE9 mouse model of Alzheimer disease. *Neurobiol Dis* 2006; **24**: 516–524.
23. Kaye R, Head E, Thompson JL, McIntire TM, Milton SC, Cotman CW *et al*. Common structure of soluble amyloid oligomers implies common mechanism of pathogenesis. *Science* 2003; **300**: 486–489.
24. Liang B, Duan BY, Zhou XP, Gong JX, Luo ZG. Calpain activation promotes BACE1 expression, amyloid precursor protein processing, and amyloid plaque formation in a transgenic mouse model of Alzheimer disease. *J Biol Chem* 2010; **285**: 27737–27744.
25. Pike CJ, Cummings BJ, Cotman CW. Early association of reactive astrocytes with senile plaques in Alzheimer's disease. *Exp Neurol* 1995; **132**: 172–179.
26. Morris RG, Garrud P, Rawlins JN, O'Keefe J. Place navigation impaired in rats with hippocampal lesions. *Nature* 1982; **297**: 681–683.
27. Toledo EM, Colombes M, Inestrosa NC. Wnt signaling in neuroprotection and stem cell differentiation. *Prog Neurobiol* 2008; **86**: 281–296.
28. Santos MS, Li H, Voglmaier SM. Synaptic vesicle protein trafficking at the glutamate synapse. *Neuroscience* 2009; **158**: 189–203.
29. Boeckers TM. The postsynaptic density. *Cell Tissue Res* 2006; **326**: 409–422.
30. Burgos PV, Mardones GA, Rojas AL, daSilva LL, Prabhu Y, Hurley JH *et al*. Sorting of the Alzheimer's disease amyloid precursor protein mediated by the AP-4 complex. *Dev Cell* 2010; **18**: 425–436.
31. Jankowsky JL, Younkin LH, Gonzales V, Fadale DJ, Slunt HH, Lester HA *et al*. Rodent A beta modulates the solubility and distribution of amyloid deposits in transgenic mice. *J Biol Chem* 2007; **282**: 22707–22720.
32. Ballatore C, Lee VM, Trojanowski JQ. Tau-mediated neurodegeneration in Alzheimer's disease and related disorders. *Nat Rev Neurosci* 2007; **8**: 663–672.
33. Brunden KR, Ballatore C, Crowe A, Smith 3rd AB, Lee VM, Trojanowski JQ. Tau-directed drug discovery for Alzheimer's disease and related tauopathies: a focus on tau assembly inhibitors. *Exp Neurol* 2009; **223**: 304–310.
34. Vincent I, Rosado M, Kim E, Davies P. Increased production of paired helical filament epitopes in a cell culture system reduces the turnover of tau. *J Neurochem* 1994; **62**: 715–723.
35. Churcher I. Tau therapeutic strategies for the treatment of Alzheimer's disease. *Curr Top Med Chem* 2006; **6**: 579–595.
36. Hooper C, Killick R, Lovestone S. The GSK3 hypothesis of Alzheimer's disease. *J Neurochem* 2008; **104**: 1433–1439.
37. Cancino GI, Perez de Arce K, Castro PU, Toledo EM, von Bernhardi R, Alvarez AR. c-Abl tyrosine kinase modulates tau pathology and Cdk5 phosphorylation in AD transgenic mice. *Neurobiol Aging* 2011; **32**: 1249–1261.
38. Noble W, Planel E, Zehr C, Olm V, Meyerson J, Suleman F *et al*. Inhibition of glycogen synthase kinase-3 by lithium correlates with reduced tauopathy and degeneration in vivo. *Proc Natl Acad Sci USA* 2005; **102**: 6990–6995.
39. Phiel CJ, Wilson CA, Lee VM, Klein PS. GSK-3 $\alpha$  regulates production of Alzheimer's disease amyloid- $\beta$  peptides. *Nature* 2003; **423**: 435–439.
40. Inestrosa NC, Arenas E. Emerging roles of Wnts in the adult nervous system. *Nat Rev Neurosci* 2010; **11**: 77–86.
41. Garrido JL, Godoy JA, Alvarez A, Bronfman M, Inestrosa NC. Protein kinase C inhibits amyloid  $\beta$  peptide neurotoxicity by acting on members of the Wnt pathway. *FASEB J* 2002; **16**: 1982–1984.
42. Inestrosa NC, Godoy JA, Quintanilla RA, Koenig CS, Bronfman M. Peroxisome proliferator-activated receptor  $\gamma$  is expressed in hippocampal neurons and its activation prevents  $\beta$ -amyloid neurodegeneration: role of Wnt signaling. *Exp Cell Res* 2005; **304**: 91–104.
43. Querfurth HW, LaFerla FM. Alzheimer's disease. *N Engl J Med* 2010; **362**: 329–344.
44. Cerpa W, Farias GG, Godoy JA, Fuenzalida M, Bonansco C, Inestrosa NC. Wnt-5a occludes A $\beta$  oligomer-induced depression of glutamatergic transmission in hippocampal neurons. *Mol Neurodegener* 2010; **5**: 3.
45. Lynch MA. Long-term potentiation and memory. *Physiol Rev* 2004; **84**: 87–136.
46. Leung LS. Kindling, long-term potentiation and spatial memory performance. *Can J Neurol Sci* 2009; **36**(Suppl 2): S36–S38.
47. Shapiro ML, Eichenbaum H. Hippocampus as a memory map: synaptic plasticity and memory encoding by hippocampal neurons. *Hippocampus* 1999; **9**: 365–384.
48. Whitlock JR, Heynen AJ, Shuler MG, Bear MF. Learning induces long-term potentiation in the hippocampus. *Science* 2006; **313**: 1093–1097.
49. Almeida CG, Tampellini D, Takahashi RH, Greengard P, Lin MT, Snyder EM *et al*. Beta-amyloid accumulation in APP mutant neurons reduces PSD-95 and GluR1 in synapses. *Neurobiol Dis* 2005; **20**: 187–198.
50. Roselli F, Tirard M, Lu J, Hutzler P, Lamberti P, Livrea P *et al*. Soluble  $\beta$ -amyloid1-40 induces NMDA-dependent degradation of postsynaptic density-95 at glutamatergic synapses. *J Neurosci* 2005; **25**: 11061–11070.
51. Walsh DM, Klyubin I, Fadeeva JV, Cullen WK, Anwyl R, Wolfe MS *et al*. Naturally secreted oligomers of amyloid  $\beta$  protein potently inhibit hippocampal long-term potentiation in vivo. *Nature* 2002; **416**: 535–539.
52. Griffith TN, Varela-Nallar L, Dinamarca MC, Inestrosa NC. Neurobiological effects of Hyperforin and its potential in Alzheimer's disease therapy. *Curr Med Chem* 2010; **17**: 391–406.



**Translational Psychiatry** is an open-access journal published by Nature Publishing Group. This work is licensed under the Creative Commons Attribution-NonCommercial-No Derivative Works 3.0 Unported License. To view a copy of this license, visit <http://creativecommons.org/licenses/by-nc-nd/3.0/>

Supplementary Information accompanies the paper on the Translational Psychiatry website (<http://www.nature.com/tp>)